F. TEHOVNIK, J. BURJA, B. ARH, F. VODE

ISSN 0543-5846
METABK 56(1-2) 63-66 (2017)
UDC – UDK 669.15.26.24.28-536.452:621.785:620.18:620.17=111

PRECIPITATION OF σ PHASE IN SUPERAUSTENITIC STAINLESS STEEL UHB 904L

Received – Primljeno: 2016-06-13
Accepted – Prihvaćeno: 2016-09-07
Original Scientific Paper – Izvorni znanstveni rad

Superaustenitic stainless steel UHB 904L with high Mo concentrations is widely used in applications that require high toughness and corrosion resistance. Given certain thermal histories, UHB 904L may be susceptible to the formation of potentially detrimental intermetallic phases, such as the σ (sigma) phase. The formation of the σ phase is promoted by high concentrations of Cr and Mo, while elements such as carbon, nickel and nitrogen retard its formation. Samples of UHB 904L were isothermally annealed within the temperature range between 850 – 1 000 °C, for 8 h each, followed by water quenching. Microstructural analyses using light and electron microscopy showed that the σ phase forms at temperatures up to 1 000 °C. The tensile specimens were solution treated at 1 000 °C, 1 060 °C, 1 100 °C and 1 140 °C for 0,5 h, followed by water quenching. The tensile tests were performed at room temperature.

Key words: stainless steel - Cr-Ni-Mo, σ phase, quenching, microstructure, mechanical properties

INTRODUCTION

The precipitation of the σ (sigma) phase, which is often observed in various series of austenitic stainless steels, is one of the main reasons for the deterioration of stainless steels properties. The presence of the σ phase not only affects the mechanical properties of the material detrimentally, but also reduces its corrosion resistance by removing chromium and molybdenum from the austenitic matrix [1,2]. Superaustenitic stainless steel UHB 904L has a high Ni content (25 wt. % Ni) and, importantly, it contains a significant amount of Mo (4 wt. % Mo) in addition to a level of Cr (20 wt. % Cr). The relatively high levels of Cr and Mo in the UHB 904L suggest the possibility of rejection of these elements to the interdendritic regions during the solidification process. When these bands contain sufficient levels of chromium and molybdenum, they are susceptible to the formation of the σ phase. Thus, the maximum susceptibility to the σ formation is usually observed near the plate centreline [3,4]. The σ phase can be precipitated during high-temperature processes like hot-rolling, welding, forging and ageing. The purpose of this study is to identify the presence of the σ phase that precipitates in UHB 904L samples during isothermal annealing and correlate it with tensile behaviour.

EXPERIMENTAL

Specimens of UHB 904L superaustenitic stainless steel were used in the study. The chemical composition and as-received microstructure of this steel are presented in Table 1 and Figure 1, respectively.

Table 1 **Chemical composition of steel / mas. %**

C	Si	Mn	Cr	Ni	Mo	Cu	N
0,006	0,22	1,41	19,61	26,1	3,9	1,4	0,068

Samples of the UHB 904L superaustenitic stainless steel were isothermally annealed within the temperature range between 850 – 1 000 °C for 8 h, followed by water quenching. The tensile specimens were prepared to the standard EN-10002-5; 1991 (DIN 50125). The tensile specimens were then solution treated at 1 000 °C, 1 060 °C, 1 100 °C and 1 140 °C for 0,5 h, followed by water quenching. The tensile tests were performed at room temperature. The tests were carried out using a 500 kN Instron static-dynamic testing machine. The cross-head speed was 5 mm/min according to the standard SIST EN ISO 6892-1:2010 B15. The specimens were metallographicaly prepared by grinding, polishing and then chemically etched using a solution HCl, HNO_3 and glycerine (3:1:2). Microphot FXA-Nikon light microscope equipped with a Hitachi HV-C20AMP 3CCD camera, and JEOL JSM-5610 SEM/EDS microscope were used for metallographic analyses.

RESULTS AND DISCUSSION

Figure 1 shows the initial microstructure of UHB 904L. The microstructure was fully austenitic with equiaxed grains, and with slightly smaller grains in the plate centre. The initial grain size was 110 μm, with a large number of annealing twins in austenite grains, typical for alloys with low stacking-fault energy. How-

F. Tehovnik, J. Burja, B. Arh, F. Vode, Institute of Metals and Technology, Ljubljana, Slovenia

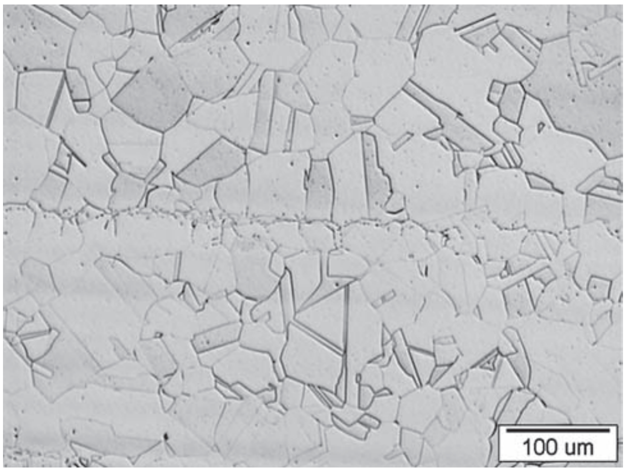

Figure 1 Initial microstructure after solution annealing with the intermetallic stringers

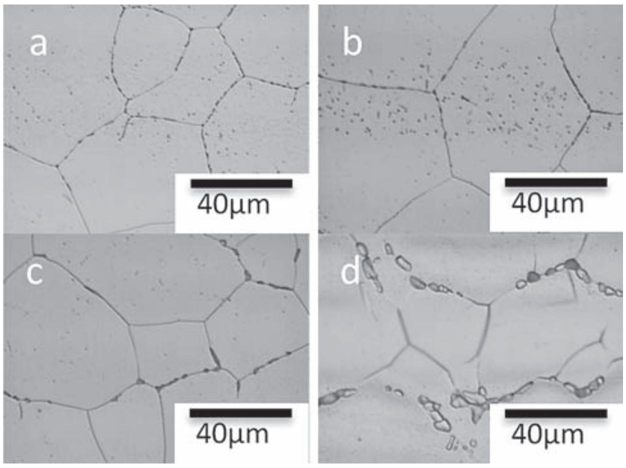

Figure 2 Morphology and distribution of σ phase in microstructure of specimens after isothermal annealing (a - 850 °C, b - 900 °C, c - 950 °C, d - 1 000 °C) for 8h

ever, in the middle of the plate, stringers of intermetallic phases were found which were elongated in the rolling direction (Figure 1). Within these solute-enriched bands, σ precipitates can form, varying in size and distribution, depending on the magnitude of the compositional segregation. Generally, the direct precipitation of σ phase in austenite is sluggish, because the σ phase contains low carbon and nitrogen, hence carbide and nitride precipitation should occur before precipitation of the σ. The diffusion of substitutional elements is very slow in austenite, and the σ phase is incoherent with austenite, therefore its nucleation is difficult [5].

The σ phase in AISI 904L forms from austenite, because the solidification is primarily austenitic, as is true for all austenitic stainless steels with the wt.($Cr_{eq.}$)/ wt.($Ni_{eq.}$) <1,5 [6,7].

Metallographic analysis of isothermally annealed specimens reveals austenite microstructure with many secondary phases observed along grain boundaries, and within grains as well [8]. Figure 2 shows LOM micrographs of specimens isothermally annealed for 8 h at different temperatures. A non-uniform distribution of σ particles along grain boundaries is observed, with varying aspect ratio dependent on temperature. The volume concentration of σ phase reached its maximum at 1 000 °C. Different morphologies of σ phase particles depend on their location; e.g., the particles at grain boundaries have a rounded shape. No differences in the chemical composition of irregular and rounded particles were observed. It may be assumed that differently shaped particles represent precipitates of one same phase, whereas the difference in their morphology is probably due to different conditions of the formation and growth at grain boundaries and within the grains.

Dendrite segregations occur due to high content of chromium and molybdenum and are possible due to variable ratio between ferrite and austenite forming elements in austenite grains. At selected temperatures σ phase precipitates at grain boundaries and in the segregation bands in the form of lamellas or irregular shapes. As can be seen from Figure 3 and the corresponding energy dispersive spectroscopy (EDS) analyses the Cr content in σ phase can reach up to 30 %, Mo contents from 15 % to 20 %, and Ni contents are below 14 %. The σ phase mostly forms at the austenite grain boundaries, triple junctions and incoherent twin border.

The segregation bands have a high density of second-phase particles that are primarily based on the σ phase. The precipitation of intermetallic phases directly from austenite is much faster in the superaustenitic material, compared to the lower alloyed stainless steels grade which require extended annealing times to form intermetallic phases [9]. As observed in the present study and as reported elsewhere [10], intermetallic phases are the first precipitates observed in superaustenitic stainless steels, while carbides are the first precipitates observed in the lower alloyed austenitic grades.

In order to retard precipitation of σ in superaustenitic stainless steels it is necessary to keep the nitrogen level high, and the carbon level low, because of the high

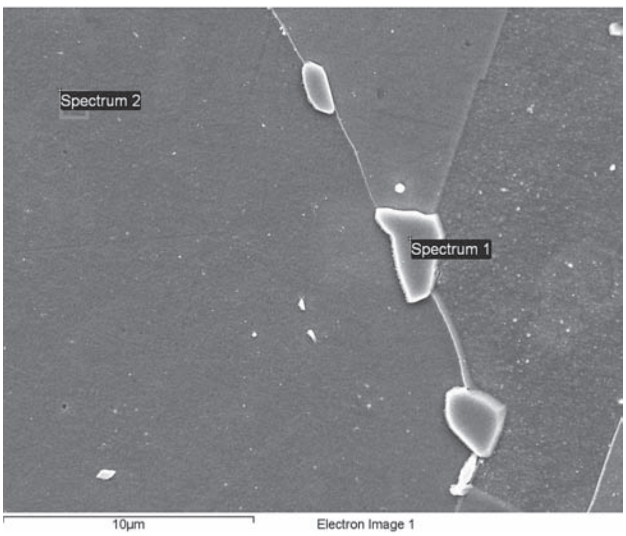

Spectrum	Cr	Mn	Fe	Ni	Cu	Mo
1	29,7	1,7	37,2	11,1		19,9
2	19,6	1,4	47,3	22,8	3,2	5,4

Figure 3 Scanning electron microscope (SEM) image and chemical composition of σ phase and matrix / mas. %

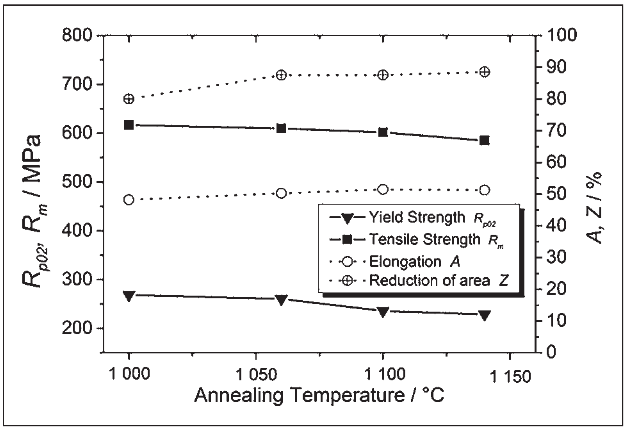

Figure 4 Mechanical properties UHB 904L as function of annealing temperature

contents of chromium and molybdenum in steel (in the present study the carbon content is <0,01 %, and that of nitrogen about 0,07 %). In comparison to nitrogen-free austenite the nitrogen alloyed austenite is more stable, because the Gibbs free energy is lower [11]. Carbon in solid solution prevents the formation of σ phase, as σ phase has a very low carbon solubility level [12]. The precipitation of the σ phase can be elimineted by the use of the solid solution heat treatment. When stainless steels UHB 904L is heated above 1 020°C, the σ phase dissolves into the γ-austenite matrix, the dissolution process is called the "$\sigma \rightarrow \gamma$ phase transformation" [13].

Figure 4 presents mechanical properties of superaustenitic stainless steel UHB 904L as a function of annealing temperature. The results show that tensile strength and yield strength decrease with the increasing temperature. At 1 000 °C, the specimens had the highest tensile strength and yield strength, which could be attributed to the fact that tensile strength and yield strength depend strongly on the grain size [14]. The elongation and reduction of area reached the maximum after annealing at 1 060, 1 100 and 1 140 °C and the minimum at the annealing temperature 1 000 °C.

Figure 5 shows SEM observations of the fracture surfaces after solution heat-treatments. Classical ductile fracture profiles with many fine and shallow dimples at the annealing temperatures between 1 060 and 1 140 °C are observed (Figures 5/b, c, d). The fracture surface after solution heat-treatment at 1 000 °C revealed a lamellar fracture profile in line of tensile deformation (Figure 5a). The nucleation of large cavities occurred at the coarse precipitates. Further investigation of cavity region showed some cleavage-like fracture. The fracture surface of the tensile specimen, shown in Figure 6**,** reveals a brittle characteristic of some coarse precipitates. Using EDS analysis the particles can be identified as σ phase. However, the secondary phases have coarsened, and became brittle and hard.

Thus, the elongation and reduction of area declined. The drop in ductility might be linked to the location of the precipitation, type of precipitation and shape of the precipitates. At the same time, some polygonal σ phases were also detected in the specimen annealed at 1 000 °C.

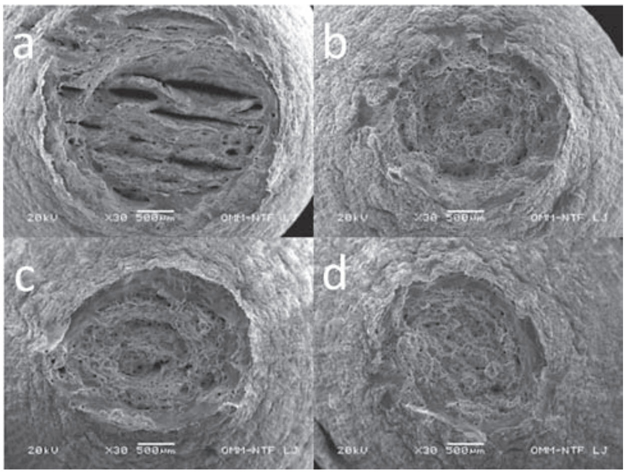

Figure 5 Scanning electron microscope (SEM) observations of the fracture surfaces after solution heat-treatments at: a – 1 000 °C, b – 1 060 °C, c – 1 100 °C, d – 1 140 °C

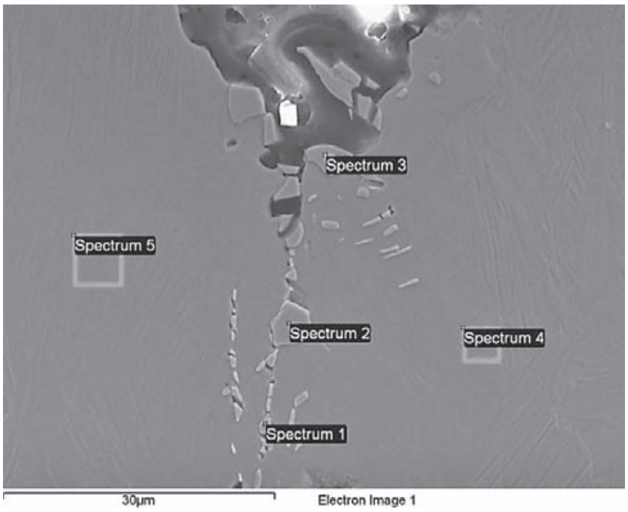

Spectrum	Cr	Mn	Fe	Ni	Cu	Mo
1	28,6	1,7	35,7	11,9		21,4
2	28,1	1,7	35,6	12,3		21,9
3	28,8	1,2	35,7	11,5		22,2
4	19,9	1,6	48,4	22,4	2,9	4,5
5	19,6	1,5	48,5	22,4	3,5	4,3

Figure 6 Scanning electron microscope (SEM) image of fractured surface and the corresponding EDS analysis (mas.%) after solution annealing at 1 000 °C

The higher content of molybdenum in UHB 904L moves the temperature range of the σ phase precipitation to higher temperatures (about 1 000 °C) [15]. During solution annealing between 1 060 and 1 140 °C the secondary phases dissolve into matrix, so the reduction in tensile strength is observed. The precipitation of σ phase was not observed in the dimples of the ductile fracture after solution annealing at 1 060, 1 100 and 1 140 °C.

CONCLUSIONS

The volume concentration of σ phase in superaustenitic stainless steel UHB 904L was the highest after annealing at 1 000 °C. During annealing σ phase precipitates at grain boundaries and in the segregation band(s) either in the form of lamellas, or irregular shapes within austenite grains. The results show that tensile strength and yield strength decrease with the increasing annealing temperature. The elongation and reduction of area reached their maximum after annealing at 1 060, 1 100 and 1 140 °C, and their minimum at 1 000 °C. During solution annealing between 1 060 and 1 140 °C the secondary phases dissolve. The precipitation of σ phase was not observed in dimples of the ductile fractures after solution annealing at 1 060, 1 100 and 1 140 °C.

REFERENCES

[1] Schwind, M.; Källqvist, J.; Nilsson, J. O.; Ågren, J.; Andrén, H. O. σ-Phase Precipitation in Stabilized Austenitic Stainless Steels. Acta Mater. 48 (2000) 10, 2473–2481.

[2] Koutsoukis, T; Redjaimia, A.; Fourlaris, G.;. Materials Science & Engineering A Phase transformations and mechanical properties in heat treated superaustenitic stainless steels. 561 (2013), 477–485.

[3] Fonda, R. W.; Lauridsen, E. M.; Ludwig, W.; Tafforeau, P.; Spanos, G. Two-dimensional and three-dimensional analyses of sigma precipitates and porosity in a superaustenitic stainless steel. Metall. Mater. Trans. A. 38 (2007) 11, 2721–2726.

[4] Stauffer, A. C.; Koss, D. A.; Mckirgan, J. B. Microstructural Banding and Failure of a Stainless Steel. Metall. Mater. Trans. A 35 (2004) 4, 1317–1324.

[5] Padilha, A. F.; Rios, P. R. Decomposition of Austenite in Austenitic Stainless Steels. ISIJ Int. 42 (2002) 4, 325–337.

[6] Suutala, N. Effect of solidification conditions on the solidification mode in austenitic stainless steels. Metall. Trans. A 14 (1983) 1, 191–197.

[7] Steiner Petrovič, D.; Klančnik, G.; Pirnat, M.; Medved, J. Differential scanning calorimetry study of the solidification sequence of austenitic stainless steel. J. Therm. Anal. Calorim. 105 (2011) 1, pp 251–257.

[8] Tehovnik, F.; Žužek, B.; Arh, B.; Burja, J.; Podgornik, B. Hot Rolling Of the Superaustenitic Stainless Steel AISI 904L. Mater. Tehnol. 48 (2014) 1, 137–140.

[9] Heino, S.; Karlsson, B. Precipitation behaviour in heat affected zone of welded superaustenitic stainless steel. Mater. Sci. Technol. 15 (1999) 1, 101–108.

[10] Heino, S. Role of Mo and W during sensitization of superaustenitic stainless steel—crystallography and composition of precipitates. Metall. Mater. Trans. A 31 (2000) 8, 1893–1905.

[11] Uggowitzer, P. J.; Magdovski, R.; Speidel, O. High nitrogen austenitic Stainless steels-Properties and new developments. La Metall. Ital. 86 (1994) 6-7

[12] Villanueva, D. M. E.; Junior, F. C. P.; Plaut, R. L.; Padilha, A. F. Comparative study on sigma phase precipitation of three types of stainless steels: austenitic, superferritic and duplex. Mater. Sci. Technol. 22 (2006) 9, 1098–1104.

[13] Badji, R.; Bouabdallah, M.; Bacroix, B.; Kahloun, C.; Bettahar, K.; Kherrouba, N. Effect of solution treatment temperature on the precipitation kinetic of σ-phase in 2205 duplex stainless steel welds. Mater. Sci. Eng. A 496 (2008) 1-2, 447–454.

[14] Offerman, S. E.; Dijk, N. H. Van; Sietsma, J.; Grigull, S.; Lauridsen, E. M.; Margulies, L.; Poulsen, H. F.; Rekveldt, M. T. Grain Nucleation and Growth During Phase Transformations. Science 298 (2002) november, 1003–1005.

[15] Jargelius-Petterson, R. F. A. Precipitation trends in highly alloyed austenitic stainless steels. Zeitschrift für Met. 89 (1998) 3, 177–183.

Note: Responsible person for English translation J. Mencinger, Zgoša, Slovenia